Research Article

Journal of Environmental Nanotechnology

Microstructural Impact of Alkaline Binders in Self-compacting Geopolymer Concrete Incorporating Sustainable Materials

M. K. Muniyasamy[1], Vigneshkumar Alagarsamy[2*], M. Dinesh Kumar[1], K. Ramesh[3], Basanth Babu K. Mohanram[4] and R. D. Sathiya[5]

[1]Department of Civil Engineering, Saveetha School of Engineering, Saveetha Institute of Medical and Technical Sciences, Chennai, TN, India
[2]Department of Civil Engineering, Mother Terasa College of Engineering and Technology, Pudukkottai, TN, India
[3]Department of Civil Engineering, PSNA College of Engineering and Technology, Dindigul, TN, India
[4]Department of Civil Engineering, Ultra College of Engineering and Technology, Ultra Nagar, Madurai, TN, India
[5]Department of Computer Science and Engineering, KLEF Deemed to be University, Guntur, Vijayawada, AP, India
Received: 30.06.2025 Accepted: 13.09.2025 Published: 30.09.2025
*eng.vigneshkumar@gmail.com

ABSTRACT

The impact of alkaline binder ratios on the microstructural properties of self-compacting geopolymer concrete (SCGC) has been investigated in this paper. Five SCGC mix designs were tested with varied alkaline binder ratios between 0.40 and 0.60, employing 50% FA and 50% GGBS as binders. The binder was introduced with a 14 M NaOH solution and superplasticizer at a rate of 9 kg/m³ together with additional water at a rate of 54 kg/m³. X-ray diffraction (XRD), Fourier transform infrared spectroscopy (FTIR), scanning electron microscopy (SEM), and energy dispersive X-ray analysis (EDAX) were used to evaluate the microstructure. The XRD analysis revealed that binder ratios of 0.50, 0.55, and 0.60 favor gel formation. In contrast, the lower binder ratios of 0.40 and 0.45 indicate a more pronounced crystalline phase and less gel formation and thus incomplete geopolymerization. The SEM and EDAX analyses showed that the particles in the SCGC are irregular and angular and have a large surface area, resulting in strong interfacial bonding and improved material performance. From the results obtained, an alkaline binder ratio of 0.50 provides an optimal balance between gel formation, microstructure uniformity, and a residual crystalline phase. The current research thus sheds light on the importance of the alkaline binder ratio to improve the properties of SCGC for use in sustainable construction.

Keywords: Sustainable construction; Alkaline binder ratio; Geopolymer concrete; Microstructural properties.

1. INTRODUCTION

Concrete is fundamental to modern construction and infrastructure, valued for its unmatched versatility, strength, and longevity (Christy *et al*. 2024a). However, the environmental impact of producing Ordinary Portland cement (OPC), the primary binding agent in standard concrete, has become a global priority (Christy *et al*. 2024b). The production process for OPC is highly energy-intensive, involving the calcination of limestone at elevated temperatures. This not only requires significant fossil fuel resources but also releases substantial amounts of carbon dioxide (CO_2) as a by-product (Christy *et al*. 2024c). Consequently, OPC production accounts for approximately 8% of global greenhouse gas emissions, making it one of the largest human-made contributors to global warming (Alagarsamy *et al*. 2025a). This concerning statistic highlights the urgent need to reduce the environmental footprint of cement production (Alagarsamy *et al*. 2025b). As a result, researchers and engineers worldwide are accelerating their efforts to find alternative materials and technologies that minimize greenhouse gas emissions while maintaining the mechanical properties, durability, and workability that make concrete a preferred building material (Maheswaran *et al*. 2023).

Among these alternatives, geopolymer concrete (GPC) has emerged as a revolutionary substitute for traditional OPC-based concrete, offering significant environmental and performance benefits (Maheswaran *et al*. 2024). It is synthesized from industrial waste materials, such as fly ash (FA) and ground granulated blast furnace slag (GGBS), which serve as aluminosilicate precursors (Wijesekara *et al*. 2025). These typically discarded wastes chemically react with alkaline activators, such as sodium hydroxide and sodium silicate, during the geopolymerization process (Ghanim *et al*. 2025). The result is a hardened binder matrix that possesses high density and strength and is highly resistant to chemical degradation (Hashem *et al*. 2025). In contrast to OPC, which relies on limestone calcination, a process that produces substantial CO_2 emissions, GPC production generates significantly lower greenhouse gases, making it as a major low-carbon construction innovation (Jalal *et al*. 2024, Sbahieh *et al*. 2025).

Beyond its ecological benefits, GPC exhibits improved mechanical properties, including high tensile and compressive strengths, enhanced sulfate and chloride resistance, and reduced shrinkage and creep (Mortada *et al*. 2025). These attributes not only enhance the material's structural efficiency but also extend the lifespan of buildings, ultimately reducing maintenance and resource consumption costs (Chen *et al*. 2024). Accordingly, GPC represents a convergence of sustainability and engineering excellence, effectively addressing the demand for sustainable materials in current infrastructure development (Salami *et al*. 2024; Zhao *et al*. 2024).

Self-compacting geopolymer concrete (SCGC) is the latest advancement in GPC technology, combining GPC's beneficial environmental properties with superior workability and flow characteristics. Unlike traditional concrete, SCGC does not require mechanical compaction when poured (Heshmati *et al*. 2025, Rawat *et al*. 2024). Its ability to flow under gravity makes it highly suitable for filling precise molds, curved shapes, and densely packed reinforcement areas, making it ideal for both prefabricated parts and large-scale civil constructions (Pradhan *et al*. 2023, Pradhan *et al*. 2022a). This flowing characteristic results in a smooth, even surface finish and minimizes the risk of voids or honeycombing, thereby improving the overall quality of the concrete (Ahmad and Zhou, 2024). Achieving optimal performance in SCGC relies on a careful balance of critical parameters, including the type and ratio of aluminosilicate precursors (e.g., FA and GGBS) and the composition of the alkaline activator solution (Shilar *et al*. 2022). The ratio and concentration of the activator, along with its interaction with the precursors, are vital for the rheological characteristics, curing behavior, and ultimate mechanical performance of the SCGC (Onyelowe *et al*. 2025). Additionally, mix design, specifically, the content of the binder and the water-to-binder ratio, significantly influences the flowability, setting time, and long-term durability of the concrete (Heweidak *et al*. 2025). Therefore, to unlock the full potential of SCGC for high-performance, durable concrete applications, a thorough understanding and optimization of these aspects are essential for achieving consistent quality and performance across different construction conditions (Tian *et al*. 2024, Mandal and Rajput, 2025).

The alkaline binder ratio is one of the most crucial factors determining the quality and performance of SCGC (Patil and Joshi, 2025). This ratio indicates the proportion of the alkaline solution relative to the total binder content, which includes industrial by-products like FA and GGBS (Kumar *et al*. 2025). This ratio plays a pivotal role in the geopolymerization process and ultimately affects the properties of the final concrete product.

This work discusses the influence of various alkaline binder ratios on SCGC microstructural properties. Five SCGC mix designs with alkaline binder ratios ranging from 0.40 to 0.60 were prepared. The mixtures were prepared in a 50:50 ratio of FA and GGBS with a Na_2SiO_3 to NaOH ratio of 1:2.5 (14 M NaOH, 9 kg/m^3 superplasticizer and 54 kg/m^3 additional water). For analyzing the microstructural characteristics, XRD, FTIR, SEM, and EDAX were used. This study identifies the optimal A/B ratio for balanced gel formation and uniform microstructure.

2. MATERIALS AND METHODS

This investigation sourced Class F FA from the coal-fired power plant, Thoothukudi, Tamil Nadu. It is a grey fine powder with a specific gravity of 2.1 and spherical in shape with a smooth surface as reflected from SEM and EDAX spectrum, as shown in Fig. 1 and 2. Ground granulated blast furnace slag, which was obtained from the JSW plant in Madurai with a specific gravity of 2.9, was added as feedstock material in geopolymer concrete. It had irregular shapes and rough surfaces as shown in Fig. 3 and 4.

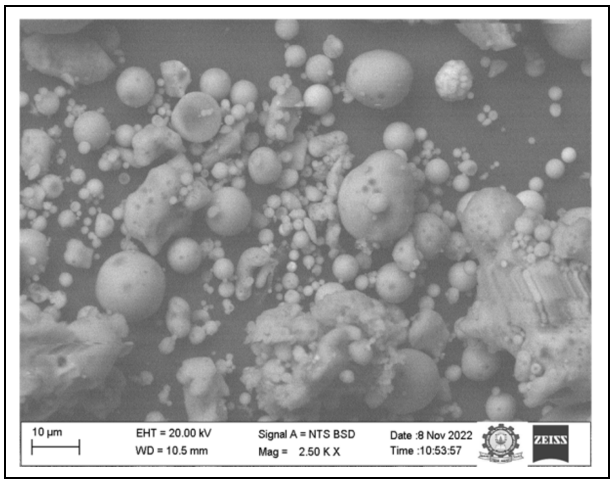


Fig. 1: SEM images of FA

The chemical composition of FA and GGBS is presented in Tables 1 and 2. From X-ray diffraction analysis (Fig. 5), it is clear that quartz and mullite are present as predominant crystalline phases of FA; while semi-crystalline phase with amorphous gypsum and calcite phases exists in GGBS as indicated by Fig. 6. The alkaline solution employed is composed of NaOH and Na_2SiO_3 in a proportion of 1:2.5, having specific gravities of 1.47 and 1.6, respectively, which were blended and stirred for 24 hours before application. Coarse aggregate with a diameter of 12.5 mm, modulus of fineness of 7.16, and specific gravity of 2.83 was utilized. The fine aggregate used is M-sand, with a specific gravity of 2.73 and a fineness modulus of 2.65. MasterGlenium Sky 8233 is a high-performance superplasticizer with a density of 1.08 g/cc and was

utilized for increasing the workability, flow, and strength of the concrete.

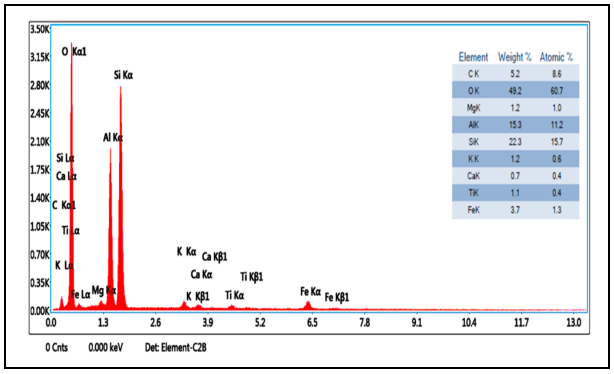


Fig. 2: Elemental compositions of FA

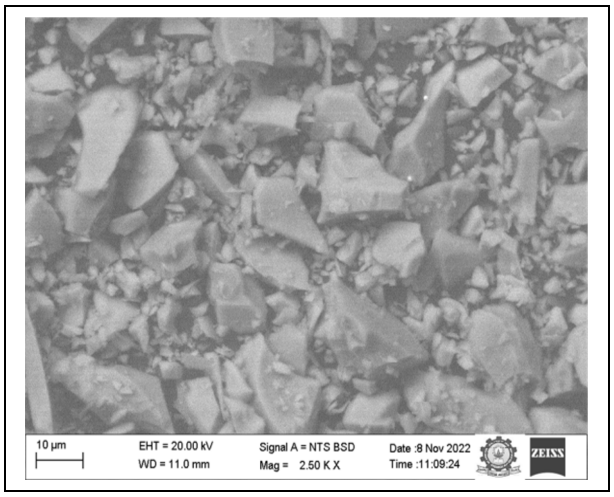


Fig. 3: SEM image of GGBS

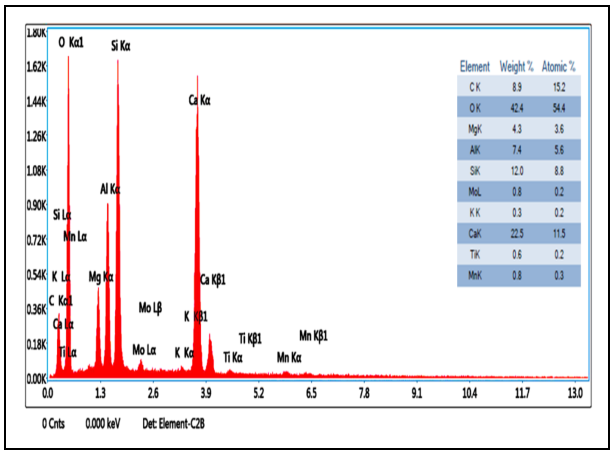


Fig. 4: Elemental composition of GGBS

In the present study, the mix ratio for SCGC consists of a total binder content of 450 kg/m^3, where the binder is a mixture of 50% FA and 50% GGBS. Sodium silicate and sodium hydroxide were used as an activator of the geopolymerization reaction. The mixture of sodium silicate and sodium hydroxide was maintained at a ratio of 1:2.5. The sodium hydroxide solution, at 14 M, contributes the alkalinity needed for the activation process. The proportion of alkali solution to binder varies between 0.40 and 0.60, depending on the desired consistency and strength. To enhance workability and reduce the amount of water used, 2% of the total binder content (9 kg/m^3) was also added as a superplasticizer that enhances the flowability and reduces the viscosity of the fresh mixture. An additional 12% water (54 kg/ m^3) was added to the mix to strengthen workability further and ensure proper mixing and pouring of the concrete. Table 3 shows the SCGC mix details.

Table 1. Chemical composition of FA

Chemical Compositions	%
SiO_2	63.16
Al_2O_3	29.69
K_2O	1.85
TiO_2	1.60
C_aO	1.41
M_gO	0.99
P_2O_5	0.97
Fe_2O_3	0.35
Na_2O	0.21
SO_3	0.16
PbO	0.02

Table 2. Chemical composition of GGBS

Chemical Compositions	%
SiO_2	35.14
Al_2O_3	16.81
K_2O	0.41
TiO_2	0.85
C_aO	37.37
M_gO	7.24
Fe_2O_3	0.07
Na_2O	0.24
SO_3	1.65
B_aO	0.10
M_nO	0.07
Cl	0.03

Table 3. SCGC mix proportions

Mix ID	Mix Proportion in kg/m^3									
	A/B Ratio	FA	GGBS	Fine Aggregate	Coarse Aggregate	NaOH	Na_2SiO_3	Molarity	SP	Extra Water
AB-1	0.40	225	225	961	786	51.43	128.57	14	9	54
AB-2	0.45	225	225	961	786	57.86	144.66	14	9	54
AB-3	0.50	225	225	961	786	64.29	160.71	14	9	54
AB-4	0.55	225	225	961	786	70.71	176.79	14	9	54
AB-5	0.60	225	225	961	786	77.14	192.86	14	9	54

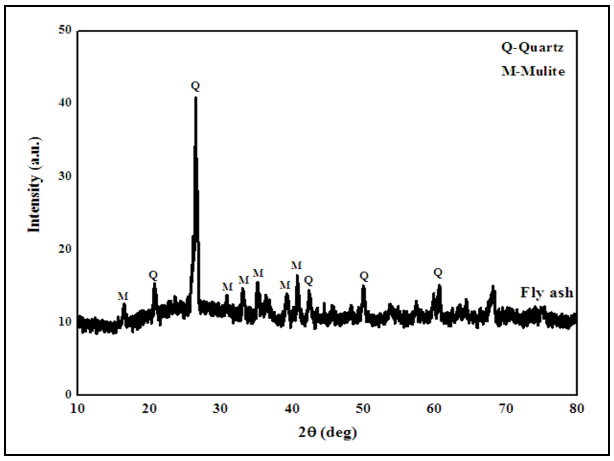


Fig. 5: XRD pattern of FA

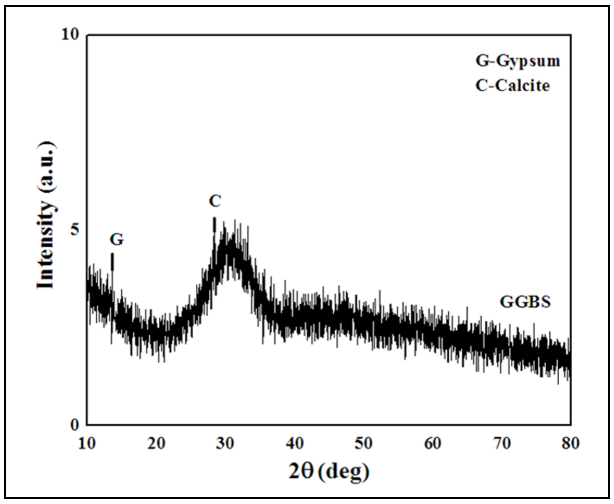


Fig. 6: XRD pattern of GGBS

2.1 Mix Proportion

The production of SCGC is a two-stage mixing process. In the first stage, FA was mixed together with GGBS and aggregates, all of which are surface-dry saturated, in a 100-litre pan mixer for about 3 minutes. This step of dry mixing ensures a good distribution of the FA, GGBS and aggregates, resulting in a homogeneous mixture. In wet mixing, which was done by adding the liquid mixture components, the mixture contained the prepared alkaline solution, superplasticizer and additional water. After mixing, the concrete was poured into moulds, and the test specimens were cured at room temperature.

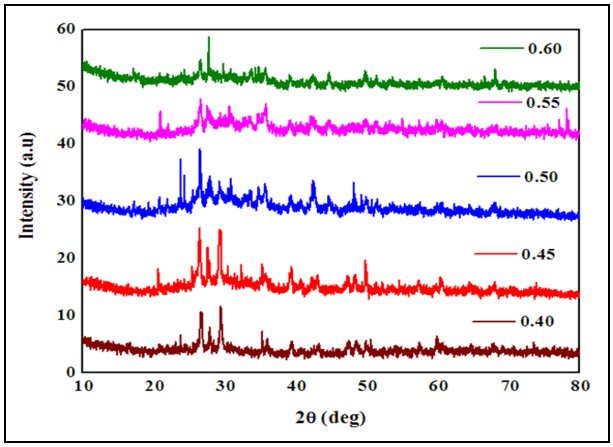


Fig. 7: XRD pattern of SCGCs with various A/B ratios 2.2 **Blending, Casting, Process, and Curing**

3. MICROSTRUCTURAL STUDIES

3.1 X-ray Diffraction

The structural and crystalline properties of the SCGCs were analyzed using a Bruker D8 Advance ECO X-ray diffraction instrument (Germany). The XRD patterns were recorded in an angular range from 10° to 80°.

3.2 Fourier Transform Infrared

An IRTracer-100 (Japan) FTIR spectrometer was used for recording spectra within the 4000–400 cm^{-1} range. The resulting spectrum is a molecular fingerprint that contains information regarding the characteristic vibrations and chemical makeup of the SCGC.

3.3 Scanning Electron Microscopy and Energy Dispersive X-ray Analysis

Scanning Electron Microscopy imaging was employed for the examination of surface morphology and microstructure of SCGCs at a binder ratio alkaline from 0.40 to 0.60 with a 2 µm resolution. Energy Dispersive X-ray Analysis was employed for examining the elemental composition by scanning the specimen with an electron beam that collides with the atoms and releases characteristic X-rays.

4. RESULTS AND DISCUSSION

4.1 XRD Analysis

The XRD patterns show the impact of alkaline binder ratios on the microstructure properties of SCCG (Fig.7), where the microstructural properties exhibited crystalline peaks corresponding to some phases like quartz and mullite, their intensities varying progressively with increased binder ratio of 0.40 to 0.60. This trend suggests a higher tendency toward the formation of amorphous gel, as suggested by the typical broad hump corresponding to aluminosilicate gels N-A-S-H in the 20° to 40° 2θ range. Higher binder ratios, like 0.50, 0.55 and 0.60, support more extensive geopolymerization, leading to denser and more homogeneous microstructures. Such samples have reduced crystalline residue and enhanced gel formation, both of which are essential for obtaining better mechanical properties and durability. On the other hand, lower binder ratios, 0.40 and 0.45, have more prominent crystalline peaks, indicating incomplete geopolymerization and the presence of unreacted precursor materials. Reduced crystallinity in higher binder ratio samples suggests better dissolution of aluminosilicate precursors and more effective polymerization. Moreover, the observed structural improvements in higher binder ratios are likely correlated with optimized silicate modulus and curing conditions, which promote the formation of a cohesive binding matrix. The general outcome of this work is that optimal binder ratios are 0.50 in enhancing the microstructural characteristics of SCGC and, hence, achieving superior performance, while balancing gel formation and minimal residual crystalline phases.

4.2 FTIR Analysis

Figs. 8 to 12 show the FTIR spectra of SCGCs with different A/B ratios: 0.40, 0.45, 0.50, 0.55, and 0.60. This shows the chemical composition and the bonding of materials. In all the spectra, a broad peak around 3440 cm^{-1} represents O-H stretching vibrations, typical of hydroxyl groups. This indicates that the sample must contain alcohols, phenols, or water. The peaks appeared at 2360-2370 cm^{-1}, corresponding to the C≡C stretching vibrations established the presence of alkynes within the material. The peaks between 1647-1797 cm^{-1} showed stretching vibration of the C=O bond, typical of carbonyl groups as found in such compounds as aldehydes, ketones, or carboxylic acids. The presence of several peaks between 1500-1000 cm^{-1} is associated with C-H bending vibrations, characteristic of many different hydrocarbon functional groups. Individual peaks at 850-871 cm^{-1} and 700-780 cm^{-1} are also related to the C-H out-of-plane bending vibrations, thus suggesting the compounds contain aromatic functional groups, with benzene rings or other structures. Overall, these spectra reveal the chemical structure of SCGCs and how variation in functional group intensities can be traced with variation in the A/B ratio.

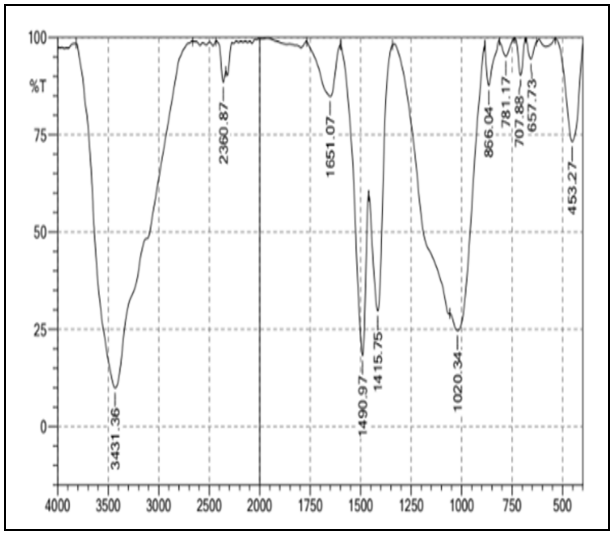


Fig. 8: FTIR spectrum of AB-1

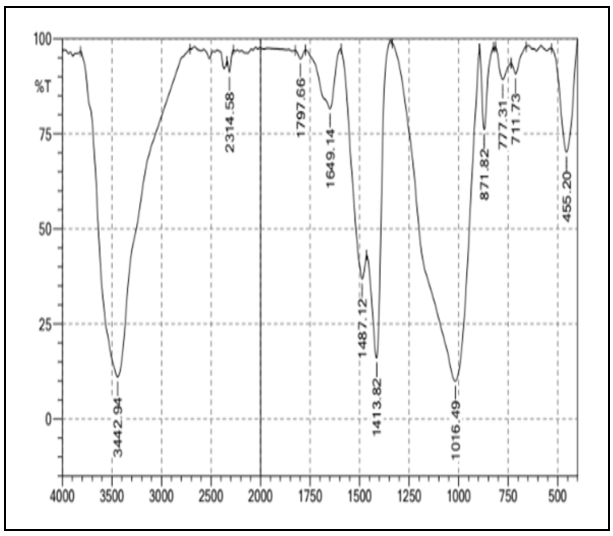


Fig. 9: FTIR spectrum of AB-2

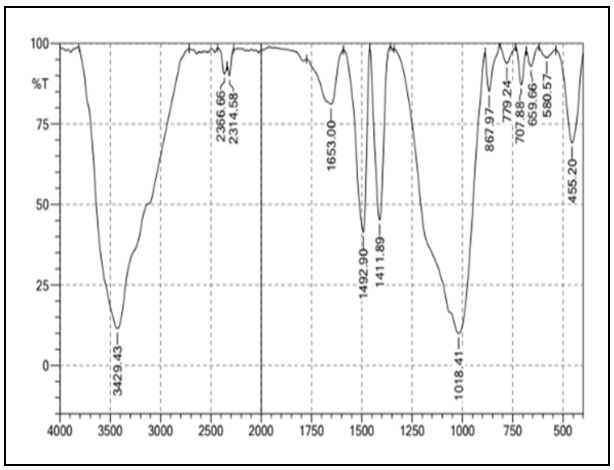


Fig. 10: FTIR spectrum of AB-3

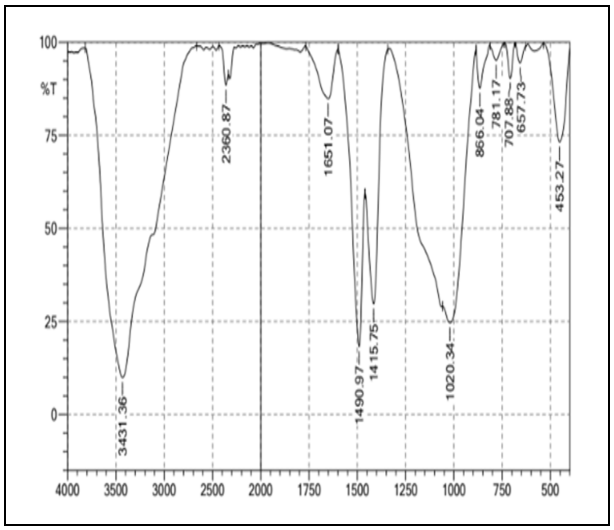


Fig. 11: FTIR spectrum of AB-4

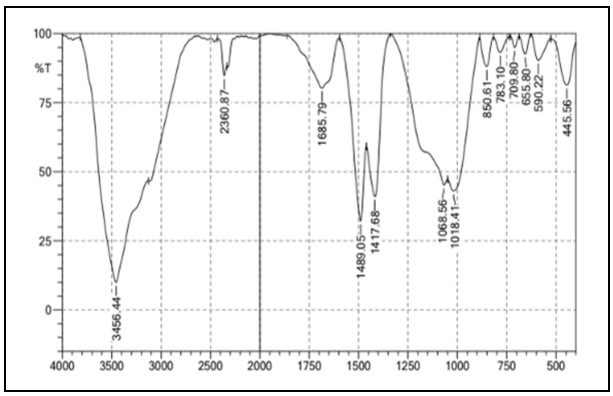


Fig. 12: FTIR spectrum of AB-5

4.3 SEM with EDAX

The SEM images in Fig. 13–17 illustrate the surface morphology of the material at different magnifications. At lower magnifications particles appear irregular and angular with rough surfaces and micro-cracks, likely due to mechanical processing such as grinding. Fig. 14 c and d show that particles are polydisperse and irregular, with micro-cracks, rough surfaces, and small spherical particles, reflecting surface irregularities. Fig.15 e and f show irregularly shaped particles with polydisperse sizes and angular rough surfaces indicating high surface energy, suitable for strong interfacial bonding. Fig. 16 g and h show heterogeneity in particle size, cracks, voids, and sharp edges, highlighting a high specific surface area for applications requiring surface interaction. Fig. 17 i and j confirm the presence of cracks, voids, and sharp edges, emphasizing the material's potential for applications demanding strong interfacial interactions and high surface reactivity.

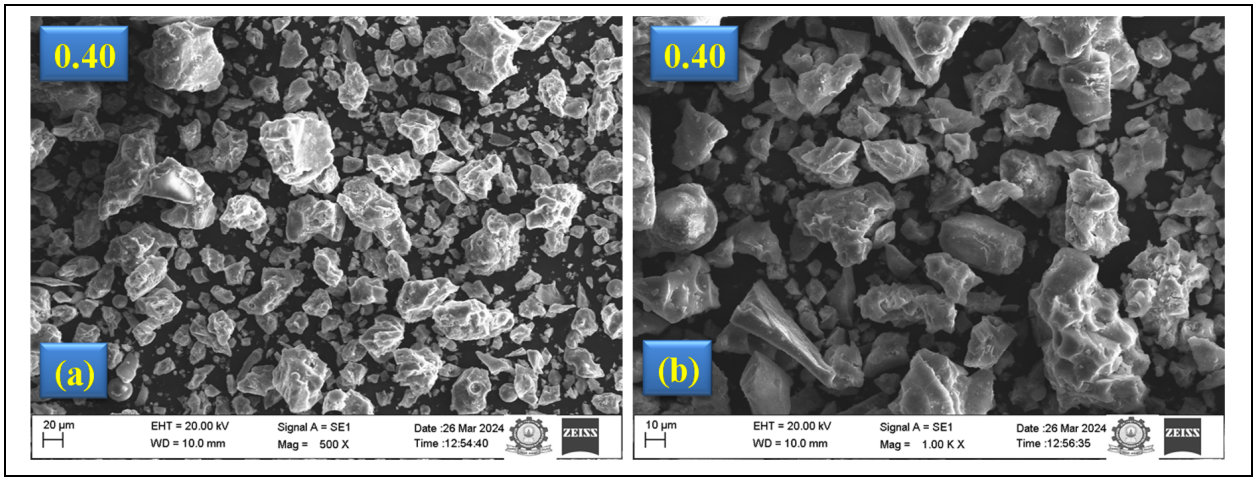


Fig. 13: (a, b) SEM image of AB-1

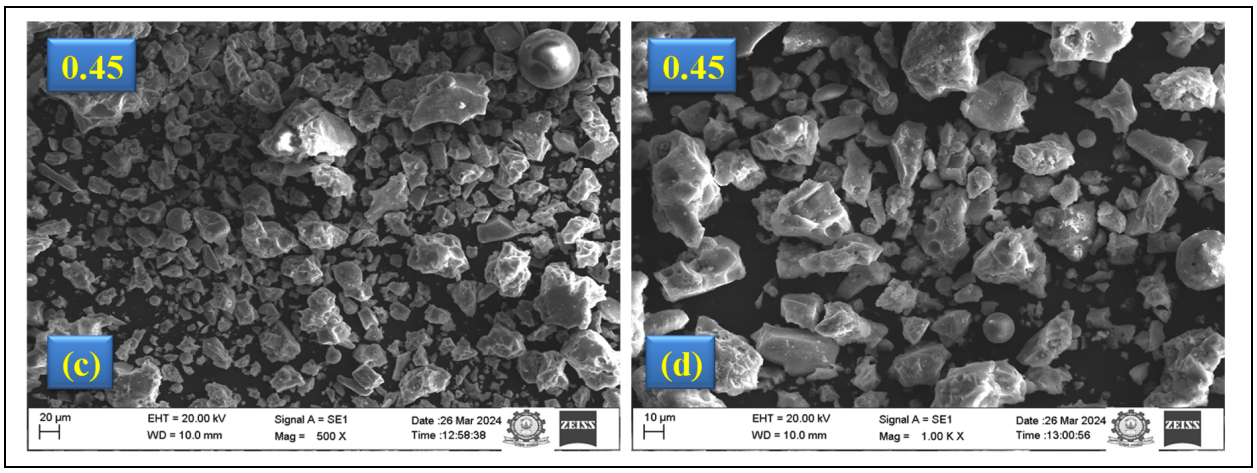


Fig. 14: (c, d) SEM image of AB-2

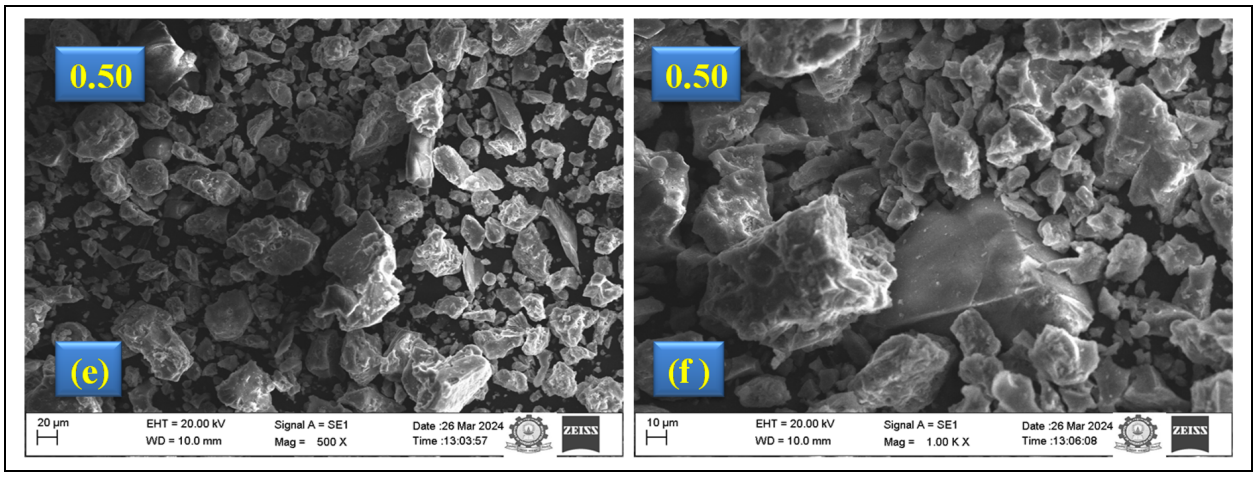


Fig. 15: (e, f) SEM image of AB-3

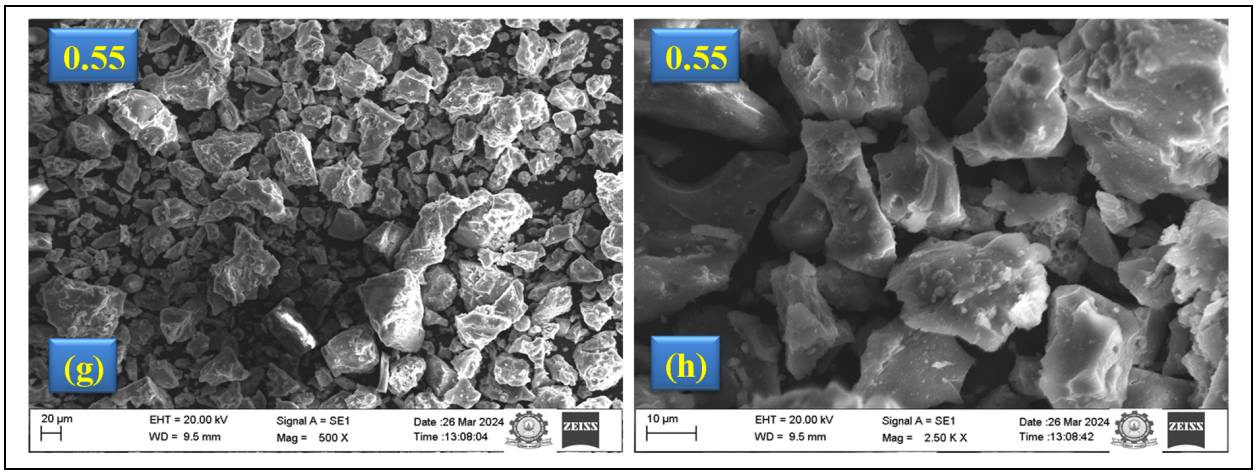


Fig. 16: (g, h) SEM image of AB-4

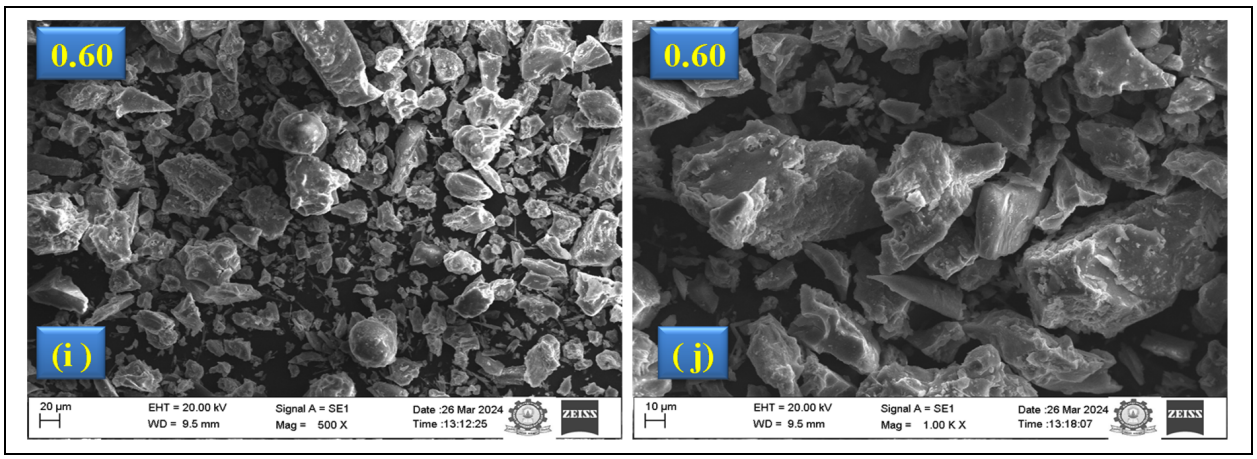


Fig. 17: (i, j) SEM image of AB-5

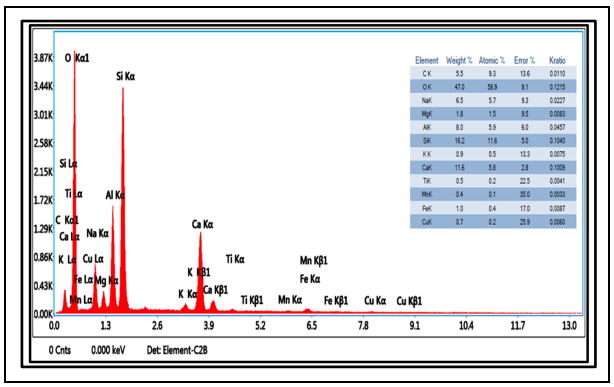


Fig. 18: EDX spectrum of AB-1

Fig. 18 shows the EDX analysis of SCGC with an A/B ratio of 0.40, highlighting the elemental composition. The material contains 16.2% Si, 6.5% Na, 8%Al, 11.6% Ca, 1% Fe, and 1.8% Mg.

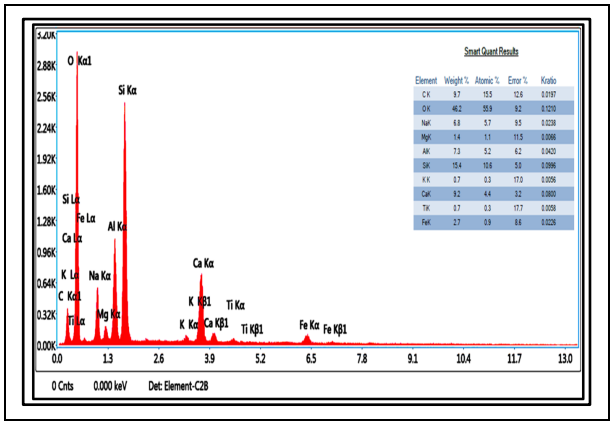


Fig. 19: EDX spectrum of AB-2

Fig. 19 shows the EDX analysis of SCGC with an A/B ratio of 0.45, displaying the elemental composition. The material contains 15.4% Si, 6.8% Na, 7.3% Al, 9.2% Ca, 2.7% Fe, and 1.4% Mg.

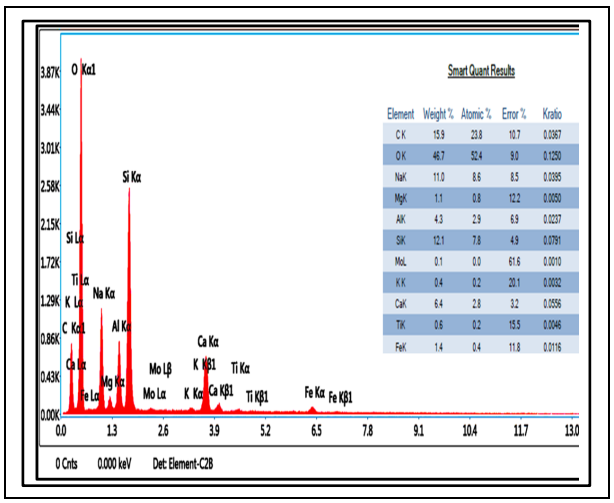


Fig. 20: EDX spectrum of AB-3

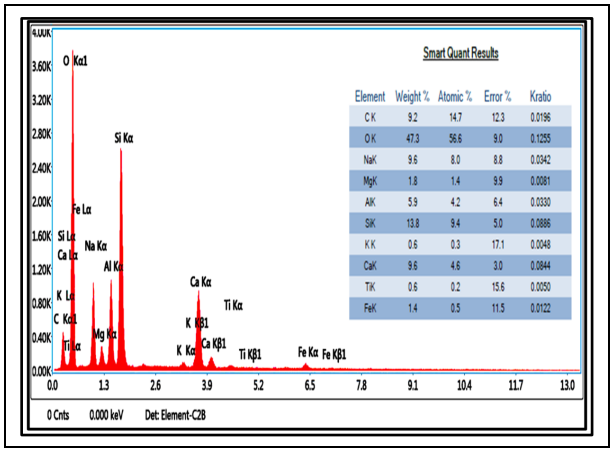


Fig. 21: EDX spectrum of AB-4

Fig. 20 shows the EDX analysis of SCGC with an A/B ratio of 0.50, highlighting the elemental composition. The material contains 12.1% Si, 11% Na, 4.3% Al, 6.4% Ca, 1.4% Fe, and 1.1% Mg.

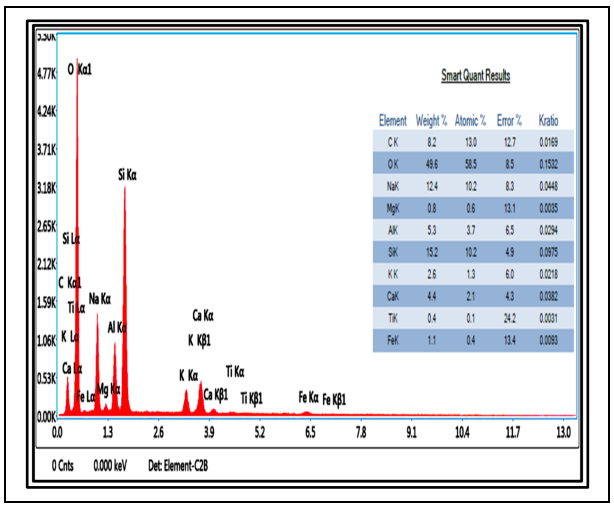


Fig. 22: EDX spectrum of AB-5

Fig. 21 shows the EDX analysis of SCGC with an A/B ratio of 0.55, displaying the elemental composition. The material contains 13.8% Si, 9.6% Na, 5.9% Al, 9.6% Ca, 1.4% Fe, and 1.8% Mg.

Fig. 22 shows the EDX analysis of SCGC with an A/B ratio of 0.60, highlighting the elemental composition. The material contains 15.2% Si, 12.4% Na, 5.3% Al, 4.4% Ca, 1.1% Fe, and 0.8% Mg.

5. CONCLUSION

This study demonstrates that higher alkaline binder ratios 0.50–0.60 significantly enhance geopolymerization, thereby improving the microstructural characteristics and performance of SCGC. The XRD analysis revealed that lower A/B ratios 0.40–0.45 showed intense crystalline peaks, indicating incomplete geopolymerization, whereas higher ratios 0.50–0.60 promoted dense, homogeneous microstructures with reduced crystallinity and increased N-A-S-H gel formation. The FTIR spectroscopy also confirmed these findings, demonstrating the presence of varying functional groups, including hydroxyl, carbonyl, and aromatic compounds whose intensities varied with the A/B ratio. The SEM images revealed that there were irregularly shaped, angular particles with a coarse surface, cracks, and voids. Particularly, the larger A/B ratios 0.50, 0.55, and 0.60 exhibited stronger crack and void development at larger magnifications, which can be the cause of a high specific surface area of the material, ideal for applications needing strong interfacial bonding. EDAX confirmed consistent major elements (Si, Na, Al, Ca, Fe) across binder ratios, with minor variations.

FUNDING DECLARATION

No funding is provided for carrying out the research work.

CONFLICTS OF INTEREST

The authors have no conflicts of interest to declare.

COPYRIGHT

This article is an open access article distributed under the terms and conditions of the Creative Commons Attribution (CC-BY) license (http://creativecommons.org/licenses/by/4.0/).

REFERENCES

Ahmad, J. and Zhou, Z., Waste marble based self compacting concrete reinforced with steel fiber exposed to aggressive environment, *J. Build. Eng*., 81, 108142 (2024). https://doi.org/10.1016/j.jobe.2023.108142

Alagarsamy, V., Christy, F. E. C., Muthiah, M. and Alengaram, J. U., Investigation of superplasticizer influence on rheological and strength properties of self-compacting geopolymer concrete, *Zast. Mater*., 66(2), 440-450(2025). https://doi.org/10.62638/ZasMat1258

Alagarsamy, V., Edwardraj, C. C. F., Muthiah, M. and Ubagaram, A. J., Influence of Alkaline Binders on the Workability and Strength of Self Compacting Geopolymer Concrete, *Zast. Mater*., 66(2), 280-291 (2025). https://doi.org/10.62638/ZasMat1181

Chen, L., Yang, M., Chen, Z., Xie, Z., Huang, L., Osman, A. I., Farghali, M., Sandanayake, M., Liu, E., Ahn, Y. H., Muhtaseb, A. H. A., Rooney, W. D. and Yap, S. P., Conversion of waste into sustainable construction materials: A review of recent developments and prospects, *Mater. Today Sustain*., 27, 100930 (2024). https://doi.org/10.1016/j.mtsust.2024.100930

Christy, A, V., C. F., Muthukannan, M. and Alengaram, U., Fresh, hardened properties and microstructural analysis on the effect of NaOH molarities of industrial by-products based self-compacting geopolymer concrete, *Int. Rev. Appl. Sci. Eng.*, 16(2), 242-264(2024a). https://doi.org/10.1556/1848.2024.00867

Christy, A, V., C. F., Muthukannan, M., Alengaram, U., Maheswaran, M. and Jeyaraj, N. J., Study of silicon dioxide nanoparticles on the rheological and mechanical behaviours of self-compacting geopolymer concrete, *Int. Rev. Appl. Sci. Eng.*, 15(3), 365-374 (2024b). https://doi.org/10.1556/1848.2024.00794

Christy, A, V., F. C., Muthukannan, M., Maheswaran, M., Arunkumar, K. and Devi, K. R., Experimental investigations on fresh and mechanical properties of fly ash and ground granulated blast furnace slag self-compacting geopolymer concrete, *Mater. Today Proc*., 96(1), 1-7 (2024c). https://doi.org/10.1016/j.matpr.2024.01.051.

Ghanim, E. A. A. H., Alengaram, J. U., Bunnori, M. N., Ibrahim, I. S. M. and Pujianiki, N. N., Exemplification of efficacy of homebrewed sodium silicate solution processed from eco-processed pozzolan and palm oil clinker powder in geopolymer mortar, *Constr. Build. Mater*., 460, 139825 (2025). https://doi.org/10.1016/j.conbuildmat.2024.139825

Hashem, S. F., Selim, F. A., Hazem, M. M., Salam, A. T. A., Monir, D. and Hassan, H. S., From waste to green binder: Valorization of industrial byproduct and natural wood fibers waste for sustainable geopolymer composite, *J. Build. Eng*., 110, 113104 (2025). https://doi.org/10.1016/j.jobe.2025.113104

Heshmati, M., Sheikh, N. M. and Hadi, S. N. M., A comprehensive review of the fresh and hardened characteristics of self-compacting geopolymer concrete, *J. Sustain. Cem. Mater.*, 14(4), 816–835 (2025). https://doi.org/10.1080/21650373.2025.2461182

Heweidak, M., Kafle, B. and Ameri, A. R., Experimental and numerical analysis of self-compacting geopolymer concrete composite slab, *Struct*., 71, 107942 (2025). https://doi.org/10.1016/j.istruc.2024.107942

Jalal, P. S., Srivastava, V. and Tiwari, A. K., Geopolymer Concrete: An Alternative to Conventional Concrete for Sustainable Construction, *J. Environ. Nanotechnol.*, 13(4), 218–225 (2024). https://doi.org/10.13074/jent.2024.12.2441122

Kanagaraj, B., Anand, N., Alengaram, U. J., R, R. S. and Jayakumar, G., Promulgation of engineering and sustainable performances of self-compacting geopolymer concrete, *J. Build. Eng.*, 68, 106093, (2023). https://doi.org/10.1016/j.jobe.2023.106093

Kumar, N. B., Reddy, M. A. and Vineela, P. S., Development of sustainable high performance self compacting concrete using construction & demolition waste and steel slag, *Discov. Civ. Eng*., 2, 62 (2025). https://doi.org/10.1007/s44290-025-00222-y

Maheswaran, M., Christy, F. C., Muthukannan, M., Arunkumar, K. and Vigneshkumar, A., Parametric study on the performance of industrial byproducts based geopolymer concrete blended with rice husk ash & nano silica, *Res. Eng. Struct. Mater*., 9(4), 1267-1285 (2023). https://doi.org/10.17515/resm2023.809ma0703

Maheswaran, M., Christy, F. C., Muthukannan, M., Arunkumar, K. and Vigneshkumar, A., Parametric Study on Strength Performance of Geopolymer Concrete Using Industrial By-Products, *Recent. Adv. Mech. Eng.*, 113–124 (2024). https://doi.org/10.1007/978-981-97-1080-5_10

Mandal, A. and Rajput, S. P. S., Advances in Alkali-Activation of Ceramic Waste-Based Pozzolana in Concrete and Mortar: A Comprehensive Review, *Waste Biomass Valorization*, 16, 3309-3330 (2025). https://doi.org/10.1007/s12649-025-02993-y

Mortada, Y., Hammoud, A., Masoud, L., Wyrzykowski, M., Sirtoli, D., Lura, P., Mansoor, B. and Masad, E., 3D Printable Ca(OH)2-based geopolymer concrete with steel fiber reinforcement, *Mater. Struct*., 58, 73 (2025). https://doi.org/10.1617/s11527-025-02600-5

Onyelowe, C. K., Ebid, M. A., Awoyera, P., Kamchoom, V., Rosero, E., Albuja, M. and Mancheno, C., Prediction and validation of mechanical properties of self-compacting geopolymer concrete using combined machine learning methods a comparative and suitability assessment of the best analysis, *Sci. Rep*., 15, 6361 (2025). https://doi.org/10.1038/s41598-025-90468-4

Panda, S. and Panigrahi, S. K., Production of sustainable GGBFS-based Self-Compacting Geopolymer Concrete containing E-waste aggregates under ambient temperature curing, *Constr. Build. Mater*., 440, 137373 (2024). https://doi.org/10.1016/j.conbuildmat.2024.137373

Parhi, S. K., Dwibedy, S. and Panigrahi, K. S., AI-driven critical parameter optimization of sustainable self-compacting geopolymer concrete, *J. Build. Eng*., 86, 108923 (2024). https://doi.org/10.1016/j.jobe.2024.108923

Patil, S. and Joshi, D. A., Experimental investigation on fresh and hardened geopolymer concrete by considering various mix design parameters, *Asian J. Civ. Eng.*, 26, 1479–1494 (2025). https://doi.org/10.1007/s42107-024-01259-7

Pradhan, J., Panda, S., Mandal, K. R. and Panigrahi, K. S., Influence of GGBFS-based blended precursor on fresh properties of self-compacting geopolymer concrete under ambient temperature, *Mater. Today Proc*., 103, 1-10 (2023). https://doi.org/10.1016/j.matpr.2023.06.338

Pradhan, P., Panda, S., Parhi, K. S. and Panigrahi, K. S., Effect of critical parameters on the fresh properties of Self Compacting geopolymer concrete, *Mater. Today Proc*., 62, 6325–6335 (2022). https://doi.org/10.1016/j.matpr.2022.02.506

Pradhan, P., Panda, S., Parhi, S. K., Panigrahi, S. K., Factors affecting production and properties of self-compacting geopolymer concrete – A review, *Constr. Build. Mater*., 344, 128174 (2022). https://doi.org/10.1016/j.conbuildmat.2022.128174

Rawat, R., Bachheti, I. and Pratap, B., F. Ash, B. Ash, Advancements in Geopolymer Concrete Technology : A Comprehensive Review of Fresh, Hardened and Microstructural Properties Material Described, *Civil Eng. Infrastruct. J*., 57(2), 269 (2024). https://doi.org/10.22059/ceij.2024.376588.2062

Salami, B. A., Bahraq, A. A., Haq, U. M. M., Ojelade, A. O., Taiwo, R., Wahab, S., Adewumi, A. A. and Ibrahim, M., Polymer-enhanced concrete: A comprehensive review of innovations and pathways for resilient and sustainable materials, *Next Mater*., 4, 100225 (2024). https://doi.org/10.1016/j.nxmate.2024.100225

Sbahieh, S., McKay, G., Nurdiawati, A. and Ghamdi, A. G. S., The sustainability of partial and total replacement of Ordinary Portland Cement: A deep dive into different concrete mixtures through life cycle assessment, *J. Build. Eng*., 108, 112830 (2025). https://doi.org/10.1016/j.jobe.2025.112830

Shilar, A. F., Ganachari, V. S., Patil, B. V., Khan, Y. M. T. and Khadar, A. D. S., Molarity activity effect on mechanical and microstructure properties of geopolymer concrete: A review, *Case Stud. Constr. Mater.*, 16, e01014 (2022). https://doi.org/10.1016/j.cscm.2022.e01014

Tian, Q., Zhou, J., Hou, J., Zhou, Z., Liang, Z., Sun, M., Hu, J. and Huang, J., Building the future: Smart concrete as a key element in next-generation construction, *Constr. Build. Mater.*, 429, 136364 (2024). https://doi.org/10.1016/j.conbuildmat.2024.136364

Venkatesan, G., Alengaram, U. J., Ibrahim, S. and Ibrahim, I. S. M., Effect of Fly Ash characteristics, sodium-based alkaline activators, and process variables on the compressive strength of siliceous Fly Ash geopolymers with microstructural properties: A comprehensive review, *Constr. Build. Mater*., 437, 136808 (2024). https://doi.org/10.1016/j.conbuildmat.2024.136808

Wijesekara, K. K. D. A., Sadique, M., Carnacina, I., Fielding, A. and Bojczuk, C. G., Mechanical and durability analysis of geopolymer concrete made with recycled silicate activator for low carbon breakwaters, *Clean. Waste Syst*., 11, 100322 (2025). https://doi.org/10.1016/j.clwas.2025.100322

Wu, H., Chen, C., Song, W. and Hou, W., High-capacity utilization of coal gangue as supplementary cementitious material, geopolymer, and aggregate: A review, *Constr. Build. Mater.*, 435, 136857 (2024). https://doi.org/10.1016/j.conbuildmat.2024.136857

Xu, H., Jiang, J. and Yang, C., Eccentric Compression Behavior of Coral Aggregate Geopolymer Concrete Columns Reinforced with Stainless-Steel Rebars, *Appl. Sci*., 15(7), 3570 (2025). https://doi.org/10.3390/app15073570

Zhao, C., Li, Z., Peng, S., Liu, J., Wu, Q. and Xu, X., State-of-the-art review of geopolymer concrete carbonation: From impact analysis to model establishment, *Case Stud. Constr. Mater*., 20, e03124 (2024). https://doi.org/10.1016/j.cscm.2024.e03124